

Electronic Supporting Information for the Article

Au-supported Pt-Au mixed atomic monolayer electrocatalyst of ultrahigh specific activity for oxidation of formic acid in acidic solution

**Zhao Huang, Yan Liu, Fangyun Xie, Yingchun Fu, Yong He, Ming
Ma, Qingji Xie* and Shouzhuo Yao***

Key Laboratory of Chemical Biology and Traditional Chinese Medicine Research (Ministry of Education of China), College of Chemistry and Chemical Engineering, Hunan Normal University, Changsha, 410081, China. Fax: +86-731-88865515; E-mail: xieqj@hunnu.edu.cn

Outline

| | |
|---|------------|
| 1. Apparatus and materials..... | S4 |
| 2. Procedures..... | S4 |
| 3. Experimental Cu_{UPD}-to-Pt replacement efficiency..... | S6 |
| 4. Experimental Cu_{UPD}-to-Au replacement efficiency..... | S7 |
| 5. Quantification of the Pt load in a Pt-Au MAMEC..... | S7 |
| 6. Comparative QCM and ICP-AES studies..... | S8 |
| Table S1..... | S11 |
| Table S2..... | S12 |
| Table S3..... | S13 |
| Table S4..... | S14 |
| Table S5..... | S15 |
| Fig. S1..... | S16 |
| Fig. S2..... | S17 |
| Fig. S3..... | S19 |
| Fig. S4..... | S20 |
| Fig. S5..... | S21 |
| Fig. S6..... | S22 |
| Fig. S7..... | S23 |
| Fig. S8..... | S24 |

| | |
|-------------------------|------------|
| Fig. S9 | S25 |
| Fig. S10 | S26 |
| Fig. S11 | S27 |
| Fig. S12 | S28 |
| Fig. S13 | S29 |
| Fig. S14 | S30 |
| References | S31 |

1. Apparatus and materials

All electrochemical experiments were carried out on a CHI660A electrochemical workstation (CH Instrument Co., USA). A conventional three-electrode electrolytic cell was used. A computer-interfaced HP4395A impedance analyzer was used in the quartz crystal microbalance (QCM) experiments. AT-cut 9 MHz piezoelectric quartz crystals (PQC) with Au electrodes (Type JA5B, Beijing Chenjing Co.) were used experimentally, and each PQC wafer was sealed on a plastic tube terminal, with one side facing solution and the other side in air. The unpolished polycrystalline gold electrode on one side of the PQC surface served as the working electrode (geometric area: 0.29 cm²). The reference electrode was a KCl-saturated calomel electrode (SCE) with a salt bridge, and a carbon rod electrode was used as the counter electrode. Uv-vis spectra were recorded on a UV2450 spectrophotometer (Shimadzu Co., Kyoto, Japan). The surface electronic structures of the Au-supported Pt-Au mixed or Pt atomic monolayer were analyzed with an X-ray photoelectron spectroscopy (XPS, K-Alpha 1063, Thermo fisher scientific, UK) equipped with a monochromatic Al K α radiation ($h\nu = 1486.6$ eV) under the base pressure of $\leq 10^{-9}$ mbar. Inductively coupled plasma atomic emission spectroscopy (ICP-AES, Baird, USA) was used to determine the load of electroplated Pt and replacement-deposited Pt using its 214.423 nm spectrum line, as discussed later.

CuSO₄·5H₂O, HCOOH, HAuCl₄·3H₂O, H₂PtCl₆·6H₂O, and K₂PtCl₄ were purchased from Tianjin Chemical Reagents Station (Tianjin, China). RuCl₃·xH₂O, RhCl₃·xH₂O, IrCl₃·xH₂O, OsCl₃·3H₂O and PdCl₂ were purchased from Tianjin Alfa Aesar Company (Tianjin, China). All chemicals were of analytical grade or better quality, and all the solutions were prepared using Milli-Q ultrapure water (Millipore, >18 M Ω ·cm).

2. Procedures

Prior to the electrochemical experiments, the Au working electrode was cleaned as follows. To remove possible surface contamination, the working electrode surface was treated with a drop of H₂SO₄ + H₂O₂ (3:1, V/V) for 3-min stay and then rinsed thoroughly with ultrapure water. After that, the working electrode was subjected to potential cycling (0–1.5 V, 30 mV·s⁻¹) in 0.2 M aqueous HClO₄ for sufficient cycles to obtain reproducible cyclic voltammograms. The treated Au

electrode could give a peak-to-peak separation of ca. 70 mV in 2 mM $\text{K}_4\text{Fe}(\text{CN})_6$ + 0.1 M Na_2SO_4 solution (-0.1–0.5 V, $50 \text{ mV}\cdot\text{s}^{-1}$), indicating a well cleaned electrode surface.

Pt atomic monolayer or Pt-Au mixed atomic monolayer modified Au electrodes were fabricated by an underpotential deposition (UPD) of Cu (Cu_{UPD})–redox replacement reaction process. A full monolayer of Cu_{UPD} was formed on an Au electrode ($\text{Cu}_{\text{UPD}}/\text{Au}$) by holding the potential at -0.01 V for 500 s in aqueous 0.1 M H_2SO_4 + 5 mM CuSO_4 (Fig. S1), except otherwise specified. After quick rinse of $\text{Cu}_{\text{UPD}}/\text{Au}$ electrode with ultrapure water, $\text{Cu}_{\text{UPD}}/\text{Au}$ was immersed in a N_2 -saturated noble metal salt solution for 900 s, allowing the redox replacement of Cu_{UPD} atoms by noble metal atoms as completely as possible. However, a QCM experiment confirmed that the Cu_{UPD} -to-Pt redox replacement reaction on the $\text{Cu}_{\text{UPD}}/\text{Au}$ electrode in 1.0 mM aqueous H_2PtCl_6 + 0.1 M HClO_4 solution (Cu_{UPD} load: $0.57 \mu\text{g}\cdot\text{cm}^{-2}$) can be finished within 3 min (see Fig. S2 with discussion details). A Pt atomic monolayer modified Au electrode is prepared by using K_2PtCl_4 (or H_2PtCl_6) as a Pt source, while a Pt-Au mixed atomic monolayer modified Au electrode with a given atomic Pt/Au ratio is prepared by varying the concentration ratio of H_2PtCl_6 to HAuCl_4 in the mixed H_2PtCl_6 + HAuCl_4 solution. Table S1 lists the corresponding noble metal salt compositions for modification of the Au electrodes and abbreviations of the prepared electrodes. For comparison, Pt-M (M=Ir, Rh, Pd, Ru, and Os) mixed atomic monolayer modified Au electrodes were similarly fabricated. The mass of noble metal atomic monolayer and the Cu_{UPD} load both in $\mu\text{g}\cdot\text{cm}^{-2}$ are calculated according to the Sauerbrey equation, $\Delta f_0 = -2.264 \times 10^{-6} f_{0g}^2 \Delta m$, where Δf_0 in Hz is the shift of the resonant frequency, Δm in $\mu\text{g}\cdot\text{cm}^{-2}$ is the areal mass change of the electrode, f_{0g} in Hz is the fundamental frequency in air (here 9.00×10^6 Hz).^{S1} After UPD of Cu in aqueous 0.1 M H_2SO_4 + 5 mM CuSO_4 , the areal Cu_{UPD} load on the Au electrode was experimentally obtained as $0.58 \pm 0.08 \mu\text{g}\cdot\text{cm}^{-2}$.

Under our experimental conditions, it is impossible to prepare a Pt-Au mixed atomic monolayer using a noble metal salt solution containing K_2PtCl_4 and HAuCl_4 , owing to the quick reduction of AuCl_4^- by PtCl_4^{2-} , as verified by QCM and UV-vis spectrophotometric experiments (see Fig. S4 with discussion details).

Commercial E-TEK Pt/C (20%) catalyst modified electrode was fabricated as follows. 1 mg

E-TEK Pt/C (20%) catalyst was ultrasonically dispersed into 1 mL ultrapure water, and 15 μL of the suspension was dropped on the surface of a glassy carbon electrode (3 mm diameter). After drying, 5 μL of 0.5 wt % Nafion alcohol solution was cast on the electrode surface, drying at room temperature before use.

The modified Au electrodes were characterized by cyclic voltammetry (CV) in 0.1 M aqueous H_2SO_4 (50 $\text{mV}\cdot\text{s}^{-1}$, -0.3–1.5 V). Electrocatalytic oxidation of formic acid was carried out by CV in aqueous 1 M HCOOH + 0.1 M H_2SO_4 (50 $\text{mV}\cdot\text{s}^{-1}$, -0.3–1.5 V). Meanwhile, chronoamperometry tests of the modified Au electrodes were investigated at 0.1 V by recording the current-time (i - t) curves of $\text{Pt}_4\text{Au}_1(\text{CuUPD-Pt}_4+)/\text{Au}$, $\text{Pt}_{(\text{CuUPD-Pt}_4+)}/\text{Au}$, $\text{Pt}_{(\text{CuUPD-Pt}_2+)}/\text{Au}$ and commercial E-TEK Pt/C (20%) for 1200 s. All of the solutions were deoxygenated by bubbling high-purity N_2 for at least 10 min prior to each measurement. The electroactive Pt surface area is estimated from the hydrogen adsorption (H UPD) charge in 0.1 M H_2SO_4 solution using a conversion factor of 210 $\mu\text{C}\cdot\text{cm}^{-2}$.^{S2}

The poison adsorption on the modified electrodes under open circuit potential and the stripping experiments were studied as described in ref. S3. Briefly, the electrode was activated by CV in 0.1 M aqueous H_2SO_4 (50 $\text{mV}\cdot\text{s}^{-1}$, -0.3–1.5 V), rinsed with ultrapure water, and immersed in 1 M aqueous HCOOH for 5 min. The electrode was then transferred to deaerated ultrapure water to remove the excess HCOOH from the electrode surface. Then, the electrode was immersed back into 0.1 M aqueous H_2SO_4 at 0 V. The adsorbed poison was stripped by scanning the potential positively within the range of -0.3–0.8 V starting at 0 V.

3. Experimental Cu_{UPD} -to-Pt replacement efficiency ($\eta_{\text{Pt-exp}}$)

The experimental Cu_{UPD} -to-Pt replacement efficiency ($\eta_{\text{Pt-exp}}$) is defined as the molar ratio of replacement-deposited Pt atoms to electrodeposited Cu_{UPD} atoms. The experimental molar quantity of replacement-deposited Pt atoms ($n_{\text{Pt-exp}}$ in $\mu\text{mol}\cdot\text{cm}^{-2}$) can be calculated from the Sauerbrey equation and the “dry” frequency shift ($\Delta f_{0-\text{Pt-exp}}$) before and after loading the Pt in each redox replacement cycle, namely, $n_{\text{Pt-exp}} = \Delta m_{\text{Pt-exp}} / 195.1 = \Delta f_{0-\text{Pt-exp}} / (-195.1 \times 2.264 \times 10^{-6} \times f_{0g}^2)$, where 195.1 in $\text{g}\cdot\text{mol}^{-1}$ is the molar weight of Pt, and f_{0g} in Hz is the fundamental frequency in air

(9.00×10^6 Hz in this work). The molar quantity of electrodeposited Cu_{UPD} atoms ($n_{\text{Cu-UPD}}$ in $\mu\text{mol}\cdot\text{cm}^{-2}$) can be calculated from the Sauerbrey equation and the frequency shift ($\Delta f_{0-\text{Cu-exp}}$) for Cu UPD, namely, $n_{\text{Cu-UPD}} = \Delta m_{\text{Cu-exp}} / 63.55 = \Delta f_{0-\text{Cu-exp}} \times 10^6 / (-63.55 \times 2.264 \times f_{0g}^2)$, where 63.55 in $\text{g}\cdot\text{mol}^{-1}$ is the molar weight of Cu. Hence,

$$\eta_{\text{Pt-exp}} = n_{\text{Pt-exp}} / n_{\text{Cu-UPD}} = \Delta f_{0-\text{Pt-exp}} \times 63.55 / (\Delta f_{0-\text{Cu-exp}} \times 195.1)$$

The $\eta_{\text{Pt-exp}}$ for $\text{Pt}_{(\text{CuUPD-Pt4+})}/\text{Au}$ (H_2PtCl_6 source) and $\text{Pt}_{(\text{CuUPD-Pt2+})}/\text{Au}$ (K_2PtCl_4 source) are calculated to be (30±3)% and (74±6)%, respectively

4. Experimental Cu_{UPD} -to-Au replacement efficiency ($\eta_{\text{Au-exp}}$)

The experimental Cu_{UPD} -to-Au replacement efficiency ($\eta_{\text{Au-exp}}$) is defined as the molar ratio of replacement-deposited Au atoms to electrodeposited Cu_{UPD} atoms. The experimental molar quantity of replacement-deposited Au atoms ($n_{\text{Au-exp}}$ in $\mu\text{mol}\cdot\text{cm}^{-2}$) can be calculated from the Sauerbrey equation and the “dry” frequency shift ($\Delta f_{0-\text{Au-exp}}$) before and after loading the Au in each redox replacement cycle, namely, $n_{\text{Au-exp}} = \Delta m_{\text{Au-exp}} / 197 = \Delta f_{0-\text{Au-exp}} / (-197 \times 2.264 \times 10^{-6} \times f_{0g}^2)$, where 197 in $\text{g}\cdot\text{mol}^{-1}$ is the molar weight of Au. In addition,

$n_{\text{Cu-UPD}} = \Delta m_{\text{Cu-exp}} / 63.55 = \Delta f_{0-\text{Cu-exp}} \times 10^6 / (-63.55 \times 2.264 \times f_{0g}^2)$. Hence,

$$\eta_{\text{Au-exp}} = n_{\text{Au-exp}} / n_{\text{Cu-UPD}} = \Delta f_{0-\text{Au-exp}} \times 63.55 / (\Delta f_{0-\text{Cu-exp}} \times 197)$$

The $\eta_{\text{Au-exp}}$ for $\text{Au}_{(\text{CuUPD-Au3+})}/\text{Au}$ (HAuCl_4 source) is calculated to be (49±3)%.

5. Quantification of the Pt load in a Pt-Au MAMEC

The Pt load in a Pt-Au mixed atomic monolayer electrocatalyst (MAMEC) is quantified by the electrochemistry plus QCM method, and the procedures are given in the following four steps. (1) A series of $\text{Pt}_{(\text{CuUPD-Pt2+})}/\text{Au}$ (or $\text{Pt}_{(\text{CuUPD-Pt4+})}/\text{Au}$) electrodes were prepared by adjusting the amount of Cu_{UPD} (0.39~0.56 $\mu\text{g}\cdot\text{cm}^{-2}$) using different applied potentials (-0.01, 0.04, 0.08, and 0.1 V vs. SCE) during UPD of Cu in aqueous 0.1 M H_2SO_4 + 5 mM CuSO_4 , followed by replacement of Cu_{UPD} with K_2PtCl_4 (or H_2PtCl_6) in aqueous 1.0 mM K_2PtCl_4 (or 1.0 mM H_2PtCl_6) + 0.1 M HClO_4 , and the Pt load for $\text{Pt}_{(\text{CuUPD-Pt2+})}/\text{Au}$ (or $\text{Pt}_{(\text{CuUPD-Pt4+})}/\text{Au}$) electrode is obtained from the QCM

frequency responses (Δf_0) and the Sauerbrey equation; (2) the prepared electrodes were subjected to potential cycling ($50 \text{ mV}\cdot\text{s}^{-1}$, -0.3 – 1.5 V) in 0.1 M aqueous H_2SO_4 to obtain data of Pt-load-dependent $|\Delta Q_{\text{Pc-Au}}|$ and H adsorption charge on Pt surface ($Q_{\text{H,UPD}}$); (3) according to the Pt load on each $\text{Pt}_{(\text{CuUPD-Pt}2+)}/\text{Au}$ (or $\text{Pt}_{(\text{CuUPD-Pt}4+)}/\text{Au}$) electrode with the corresponding $|\Delta Q_{\text{Pc-Au}}|$ and $Q_{\text{H,UPD}}$, the linear plots of the Pt load versus $|\Delta Q_{\text{Pc-Au}}|$ or $Q_{\text{H,UPD}}$ are drawn to obtain the Pt load- $|\Delta Q_{\text{Pc-Au}}|$ and Pt load- $Q_{\text{H,UPD}}$ linear regression equations, as shown in Fig. S6; (4) we use the linear regression equations to quantify the Pt load in an Au-supported Pt-Au MAMEC, after determining $|\Delta Q_{\text{Pc-Au}}|$ and $Q_{\text{H,UPD}}$ of a Pt-Au MAMEC by potential cycling ($50 \text{ mV}\cdot\text{s}^{-1}$, -0.3 – 1.5 V) in 0.1 M aqueous H_2SO_4 , as shown in Fig. S3. The Pt load of $\text{Pt}_9\text{Au}_{1(\text{CuUPD-Pt}4+)}/\text{Au}$, $\text{Pt}_4\text{Au}_{1(\text{CuUPD-Pt}4+)}/\text{Au}$ and $\text{Pt}_3\text{Au}_{1(\text{CuUPD-Pt}4+)}/\text{Au}$ are listed in Table S3.

6. Comparative QCM and ICP-AES studies

We have carefully conducted comparative in-situ QCM and ex-situ ICP-AES experiments below to measure the load of electroplated Pt and replacement-deposited Pt, in order to check the reliability of our in-situ QCM method. It should be noted that the inevitable solution-dilution effect during sample preparation for ex-situ ICP-AES assay might make the ICP-AES method less sensitive to detect the (sub)monolayer Pt load on a conventional QCM/Au electrode, thus electroplated Pt of increased load and roughened QCM/Au electrodes capable of loading more replacement-deposited Pt are employed here.

The detailed procedures for experiments of electroplated Pt are given as follows. (1) We conducted potentiostatic electroplating of Pt at -0.2 V vs. SCE on several QCM Au electrodes ($\text{Pt}_{\text{pla}}/\text{Au}$) in $2.0 \text{ mM H}_2\text{PtCl}_6 + 0.1 \text{ M HClO}_4$ solution at varying electroplating time, and the Pt load for the $\text{Pt}_{\text{pla}}/\text{Au}$ electrodes was obtained from the QCM frequency responses (Δf_0) and the Sauerbrey equation (2 min for $14.0 \mu\text{g}\cdot\text{cm}^{-2}$ Pt, 7 min for $45.0 \mu\text{g}\cdot\text{cm}^{-2}$ Pt, 22 min for $167 \mu\text{g}\cdot\text{cm}^{-2}$ Pt, and 47 min for $337 \mu\text{g}\cdot\text{cm}^{-2}$ Pt). (2) The Pt load for the $\text{Pt}_{\text{pla}}/\text{Au}$ electrodes was then determined by the ICP-AES method. Experimentally, $80 \mu\text{L}$ of fresh prepared aqua regia (3:1, $V_{\text{HCl}}/V_{\text{HNO}_3}$. Highly corrosive, treat with great care) was cast on the electrode surface for 5 min to dissolve Pt and Au, and the solution was then transferred into a tumbler. Repeating the

noble-metal-dissolution process for 10 times can fully dissolve the Pt and Au (relatively thick Pt films here), and the total volume of aqua regia used for the dissolution was 0.8 mL. After diluting the aqua regia to 10 mL by carefully adding 9.2 mL ultrapure water, the obtained solution was fed into an ICP-AES instrument (Baird, USA) to determine the concentrations of Pt by using a proper calibration curve. Thus, the Pt load at Pt_{pla}/Au electrodes can be obtained as the product of the ICP-AES-revealed Pt concentration and the solution volume (10 mL). (3) The linear plot of Pt load_{ICP-AES} (determined by ICP-AES technology) versus Pt load_{QCM} (determined by QCM method) is drawn in Fig. S7. The linear regression equation gives a Pt load_{ICP-AES}/Pt load_{QCM} ratio of almost 1:1, confirming the accuracy of QCM method in determining the Pt load.

The detailed procedures for experiments of replacement-deposited Pt on roughened QCM Au electrodes are given as follows. (1) The Au_{pla}/Au electrodes were fabricated via potentiostatically depositing Au on the QCM Au electrode at -0.2 V vs. SCE in aqueous 1 mM HAuCl₄ + 0.1 M H₂SO₄ for 3 min by two times, and the total frequency shift for Au deposits was -5.00 kHz. By using a conversion factor of 386 μC cm⁻²,^{R10} the real surface area of the as-prepared Au_{pla}/Au electrode is calculated to be 1.61 cm² and the roughness factor (a ratio of the real surface area to the geometric area of 0.29 cm²) was 5.54 on Au_{pla}/Au, after determining the reduction charge of Au oxides by potential cycling (50 mV·s⁻¹, -0.3–1.5 V vs. SCE) in 0.1 M aqueous H₂SO₄, as shown in Fig. S8. (2) UPD of Cu on Au_{pla}/Au electrode was performed at 0 V vs. SCE (about 10 mV positive of that on bare Au) in aqueous 0.1 M H₂SO₄ + 5 mM CuSO₄ for 500 s, followed by replacement of the Cu_{UPD} with K₂PtCl₄ (or H₂PtCl₆) in aqueous 1.0 mM K₂PtCl₄ (or 1.0 mM H₂PtCl₆) + 0.1 M HClO₄, the obtained electrode is denoted as Pt_{(CuUPD-Pt2+)/Au_{pla}/Au} (or Pt_{(CuUPD-Pt4+)/Au_{pla}/Au}). The Pt load on Pt_{(CuUPD-Pt2+)/Au_{pla}/Au} (or Pt_{(CuUPD-Pt4+)/Au_{pla}/Au}) is obtained from the QCM frequency responses (Δf_0) and the Sauerbrey equation. (3) The Pt load for Pt_{(CuUPD-Pt2+)/Au_{pla}/Au} (or Pt_{(CuUPD-Pt4+)/Au_{pla}/Au}) electrode was determined by the ICP-AES technology. The process is similar to those for determining the Pt load on Pt_{pla}/Au electrodes, except that the total volume of final sample solution was 5.00 mL, including 0.24 mL of aqua regia used for dissolution of the monolayer-Pt deposits and 4.76 mL of ultrapure water used for solution-dilution. Table S4 lists the Pt load of Pt_{(CuUPD-Pt2+)/Au_{pla}/Au} and Pt_{(CuUPD-Pt4+)/Au_{pla}/Au}. For each electrode, the Pt load determined by in-situ QCM method agrees acceptably with the one

determined by ex-situ ICP-AES, validating the in-situ QCM method for reliably quantifying the Pt load in the (sub)monolayer level.

Table S1. Noble metal salt compositions for preparing the modified Au electrodes

| | $c_{\text{Pt}} : c_{\text{Au}}$ | Noble metal salt composition |
|--|---------------------------------|--|
| $\text{Pt}_{(\text{CuUPD-Pt}^{2+})}/\text{Au}$ | | 1.0 mM K_2PtCl_4 + 0.1 M HClO_4 |
| $\text{Pt}_{(\text{CuUPD-Pt}^{4+})}/\text{Au}$ | | 1.0 mM H_2PtCl_6 + 0.1 M HClO_4 |
| $\text{Pt}_9\text{Au}_1(\text{CuUPD-Pt}^{4+})/\text{Au}$ | 9 : 1 | 0.9 mM H_2PtCl_6 + 0.1 mM HAuCl_4 + 0.1 M HClO_4 |
| $\text{Pt}_4\text{Au}_1(\text{CuUPD-Pt}^{4+})/\text{Au}$ | 4 : 1 | 0.8 mM H_2PtCl_6 + 0.2 mM HAuCl_4 + 0.1 M HClO_4 |
| $\text{Pt}_3\text{Au}_1(\text{CuUPD-Pt}^{4+})/\text{Au}$ | 3 : 1 | 0.75 mM H_2PtCl_6 + 0.25 mM HAuCl_4 + 0.1 M HClO_4 |
| $\text{Au}_{(\text{CuUPD-Au}^{3+})}/\text{Au}$ | | 1.0 mM HAuCl_4 + 0.1 M HClO_4 |

Table S2. Binding energies (BEs) of 4f signals for Pt⁰ and Au⁰ on the modified Au electrodes.

| | BE (eV) | | | |
|---|---------------------|---------------------|---------------------|---------------------|
| | Pt4f _{7/2} | Pt4f _{5/2} | Au4f _{7/2} | Au4f _{5/2} |
| Pt _(CuUPD-Pt2+) /Au | 71.12 | 74.36 | 83.85 | 87.57 |
| Pt _(CuUPD-Pt4+) /Au | 71.01 | 74.33 | 83.93 | 87.59 |
| Pt ₉ Au _{1(CuUPD-Pt4+)} /Au | 70.97 | 74.29 | 84.03 | 87.69 |
| Pt ₄ Au _{1(CuUPD-Pt4+)} /Au | 70.87 | 74.16 | 84.08 | 87.71 |
| Pt ₃ Au _{1(CuUPD-Pt4+)} /Au | 70.84 | 74.09 | 84.11 | 87.80 |
| Bulk metal ^a | 71.20 | 74.50 | 83.80 | 87.45 |

a: data obtained from the handbook of X-ray photoelectron spectroscopy.^{S5}

Table S3. Pt load of Au-supported Pt-Au MAMECs calculated from the Pt load- $|\Delta Q_{\text{PC-Au}}|$ and Pt load- $Q_{\text{H,UPD}}$ linear regression equations as shown in Fig. S6, respectively.

| | | Pt load ($\mu\text{g}\cdot\text{cm}^{-2}$) | | |
|--------------------------------------|--------------------------|--|--|--|
| | | $\text{Pt}_9\text{Au}_{1(\text{CuUPD-Pt}^{4+})}/\text{Au}$ | $\text{Pt}_4\text{Au}_{1(\text{CuUPD-Pt}^{4+})}/\text{Au}$ | $\text{Pt}_3\text{Au}_{1(\text{CuUPD-Pt}^{4+})}/\text{Au}$ |
| Pt load- $ \Delta Q_{\text{PC-Au}} $ | $Y = 0.0038X^{\text{a}}$ | 0.23 | 0.16 | 0.11 |
| | $Y = 0.0041X^{\text{b}}$ | 0.25 | 0.17 | 0.12 |
| Pt load- $Q_{\text{H,UPD}}$ | $Y = 0.017X^{\text{a}}$ | 0.22 | 0.14 | 0.10 |
| | $Y = 0.018X^{\text{b}}$ | 0.24 | 0.15 | 0.11 |
| Average Pt load | | 0.24 | 0.16 | 0.11 |

^a the linear regression equations for $\text{Pt}_{(\text{CuUPD-Pt}^{2+})}/\text{Au}$ electrode;

^b the linear regression equations for $\text{Pt}_{(\text{CuUPD-Pt}^{4+})}/\text{Au}$ electrode.

Table S4. Pt load of $\text{Pt}_{(\text{CuUPD-Pt}^{2+})}/\text{Au}_{\text{pla}}/\text{Au}$ and $\text{Pt}_{(\text{CuUPD-Pt}^{4+})}/\text{Au}_{\text{pla}}/\text{Au}$ obtained from the in-situ QCM and ex-situ ICP-AES methods.

| Electrode | Pt load ($\mu\text{g}\cdot\text{cm}^{-2}$) | Pt load _{QCM} ($\mu\text{g}\cdot\text{cm}^{-2}$) | Pt load _{ICP-AES} ($\mu\text{g}\cdot\text{cm}^{-2}$) |
|---|---|--|--|
| $\text{Pt}_{(\text{CuUPD-Pt}^{2+})}/\text{Au}_{\text{pla}}/\text{Au}$ | | 1.93 | 2.12 |
| $\text{Pt}_{(\text{CuUPD-Pt}^{4+})}/\text{Au}_{\text{pla}}/\text{Au}$ | | 0.82 | 0.90 |

Table S5. Electrochemical performance of some typical Pt-based catalysts toward formic acid electrooxidation[‡]

| Catalyst fabrication ^a | Investigated solution | Potential range of CV (V) | Scan rate (mV s ⁻¹) | SECA _a (mA·cm _{Pt} ⁻²) | SECA _m (mA·μg _{Pt} ⁻¹) | Reference |
|---|--|---------------------------|---------------------------------|--|--|-----------|
| Pt _{0.10} [^] Au-1.9 nm/C | 2 M HCOOH + 0.5 M H ₂ SO ₄ | -0.2 to 1.0 vs. SCE | 20 | 3.19 | 7.5 | S6 |
| nps-Pt ₆₀ Au ₄₀ /C | 0.5 M HCOOH + 0.5 M H ₂ SO ₄ | -0.2 to 1.0 vs. SCE | 50 | 2.49 | 0.56 | S7 |
| Pt _{0.10} [^] Au-3.0 nm/C | 2 M HCOOH + 0.5 M H ₂ SO ₄ | -0.2 to 1.0 vs. SCE | 20 | 1.41 | 3.1 | S8 |
| Pt-around-Au/C | 0.5 M HCOOH + 0.5 M H ₂ SO ₄ | 0 to 1.2 vs. RHE | 50 | 1.48 | 1.2 | S9 |
| PtAu alloy/C | 0.5 M HCOOH + 0.5 M H ₂ SO ₄ | 0 to 1.2 vs. RHE | 50 | 28.6 | 5.9 | S10 |
| <i>fcc</i> -Fe ₄₃ Pt ₃₇ Au ₂₀ /C | 0.5 M HCOOH + 0.5 M H ₂ SO ₄ | -0.2 to 0.9 vs. Ag/AgCl | 50 | 13.1 | 2.8 | S11 |
| Pt _(CuUPD-Pt4+) /Au | 1 M HCOOH + 0.1 M H ₂ SO ₄ | -0.3 to 1.0 vs. SCE | 50 | 28.7 | 26 | this work |
| Pt ₉ Au ₁ (CuUPD-Pt4+)/Au | 1 M HCOOH + 0.1 M H ₂ SO ₄ | -0.3 to 1.0 vs. SCE | 50 | 69.5 | 63 | this work |
| Pt ₄ Au ₁ (CuUPD-Pt4+)/Au | 1 M HCOOH + 0.1 M H ₂ SO ₄ | -0.3 to 1.0 vs. SCE | 50 | 124 | 102 | this work |
| Pt ₃ Au ₁ (CuUPD-Pt4+)/Au | 1 M HCOOH + 0.1 M H ₂ SO ₄ | -0.3 to 1.0 vs. SCE | 50 | 103 | 92 | this work |

[‡]Partial data are given based on calculation from the reported original data. Note that the strict performance comparison of the electrocatalysts is difficult, owing to the different experimental conditions (e.g., concentration of formic acid, scan rate, pH of the solution) existing in the literatures. However, our electrocatalysts have SECA_m and SECA_a higher than some reported electrocatalysts already with superior performance (as listed here, though their experimental conditions are not strictly the same) by ca. 1~2 orders of magnitude, implying the highest specific activity of our electrocatalyst reported to date. Similar performance comparison among the electrocatalysts is also adopted by other researchers.^{S6}

^a nps: nanoporous; *fcc*: face-centered tetragonal; Pt_{0.10}[^]Au-1.9nm: 1.9 nm Pt-on-Au nanoparticle with an atomic Pt/Au ratio of 0.10; C: Vulcan XC-72 carbon except for *fcc*-Fe₄₃Pt₃₇Au₂₀/C with Ketjen carbon.

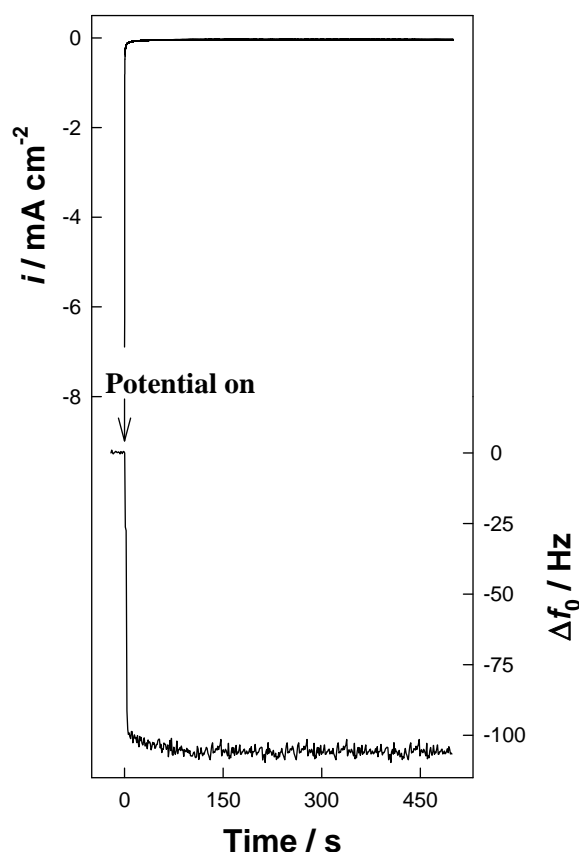


Fig. S1. Simultaneous responses of current and Δf_0 for UPD of Cu on QCM Au electrode in aqueous 0.1 M H₂SO₄ + 5 mM CuSO₄. Potential was held at -0.01 V vs. SCE for 500 s. Here, the frequency response became steady after 200 s and a steady-state frequency decrease of -105 Hz due to UPD of monolayer Cu was observed. Please note that, if bulk deposition of Cu occurred here, the frequency should decrease continuously all the time, but the frequency kept almost constant from 200 to 500 s, indicating the negligible deposition of bulk Cu here. The areal Cu_{UPD} load ($\Delta m_{\text{Cu-exp}}$ in $\mu\text{g}\cdot\text{cm}^{-2}$) can thus be calculated from the Sauerbrey equation and the frequency shift here, i.e. $\Delta f_{0-\text{Cu-exp}} = -105 = -2.264 \times 10^{-6} \times f_{0\text{g}}^2 \times \Delta m_{\text{Cu-exp}}$, where $f_{0\text{g}}$ in Hz is the fundamental frequency in air (9.00×10^6 Hz in this work). Then we obtain $\Delta m_{\text{Cu-exp}} = 0.57 \mu\text{g}\cdot\text{cm}^{-2}$.

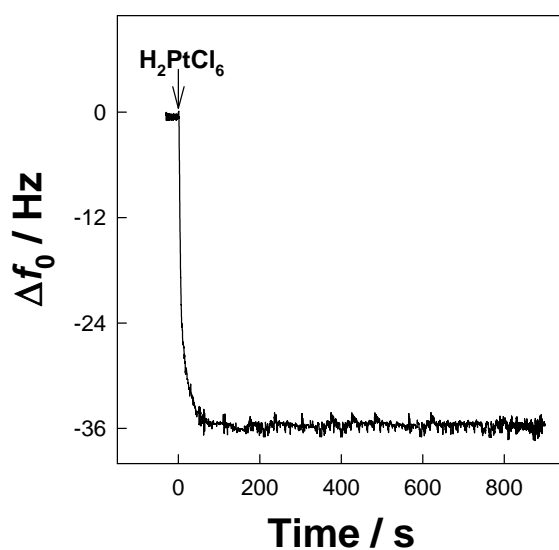


Fig. S2. Time-dependent frequency responses on $\text{Cu}_{\text{UPD}}/\text{Au}$ electrode during Cu_{UPD} -to-Pt redox replacement reaction in 1.0 mM aqueous H_2PtCl_6 + 0.1 M HClO_4 solution (H_2PtCl_6 was added at 0 s). Cu load from UPD experiment of Cu is $\Delta m_{\text{Cu-exp}} = 0.57 \mu\text{g}\cdot\text{cm}^{-2}$ (Fig. S1). After the baseline became stable in aqueous 0.1 M HClO_4 , we added 1.0 mM aqueous H_2PtCl_6 + 0.1 M HClO_4 (final concentration). Due to the replacement of remaining Cu_{UPD} with heavier Pt atoms (see below), the frequency decreased rapidly at first and tended to be stable within ca. 3 min (a total frequency decrease by -36 Hz), indicating that the replacement of Cu_{UPD} with Pt occurred rather rapidly here. The frequency kept almost steady from 3 to 15 min, indicating that the possible spontaneous deposition of $\text{Pt}^{\text{S12, S13}}$ on the QCM Au electrode in the H_2PtCl_6 + 0.1 M HClO_4 aqueous solution was negligible under our experimental conditions, and the use of 900-s redox-replacement time here will thus not result in detectable systematic experimental errors

Furthermore, we have confirmed the quantitative rationality of the observed frequency decrease ($\Delta f_{0,\text{Obs}}$, -36 Hz) after the Cu_{UPD} -to-Pt replacement (Fig. S2), by comparing the areal Pt load on Au electrode deduced from the $\Delta f_{0,\text{Obs}}$ with that obtained from the frequency responses from separate experiments ($\Delta f_{0,\text{Pt-exp}}$, see below).

(1) The areal Pt load obtained experimentally from separate “dry”-frequency QCM experiments ($\Delta m_{\text{Pt-exp}}$ in $\mu\text{g}\cdot\text{cm}^{-2}$) can be calculated from the Sauerbrey equation and the “dry” frequency shift ($\Delta f_{0,\text{Pt-exp}}$, -99 Hz in the experiments relevant to Figs. S1 and S2, measured in air) on the Au electrode before and after loading the Pt atoms by the Cu_{UPD} -to-Pt redox replacement process, i.e.,

$$\Delta f_{0-\text{Pt-exp}} = -2.264 \times 10^{-6} \times f_{0g}^2 \times \Delta m_{\text{Pt-exp}} = -99. \quad \text{We then obtain}$$

$$\Delta m_{\text{Pt-exp}} = -99 / (-2.264 \times 10^{-6} \times 9000000^2) = 0.54 \mu\text{g}\cdot\text{cm}^{-2}.$$

(2) The redox replacement reaction is $2\text{Cu} + \text{PtCl}_6^{2-} = 2\text{Cu}^{2+} + 6\text{Cl}^- + \text{Pt}$ for the H_2PtCl_6 source, and the redox displacement of Cu_{UPD} remaining at the electrode with heavier Pt atoms will lead to the mass increase of the deposit, as reflected by the observed steady-state frequency decrease ($\Delta f_{0,\text{Obs}} = -36$ Hz) in Fig. S2. Thus, the net increase of areal mass ($\Delta m_{\text{net-inc}}$) on the electrode can be estimated from the Sauerbrey equation and $\Delta f_{0,\text{Obs}}$ (-36 Hz) in Fig. S2, i.e., $\Delta f_{0,\text{Obs}} = -2.264 \times 10^{-6} \times f_{0g}^2 \times \Delta m_{\text{net-inc}}$. Hence, the expected areal Pt load ($\Delta m_{\text{Pt-Exptd}}$) on Au electrode can be calculated according to $\Delta m_{\text{Pt-Exptd}} = \Delta m_{\text{net-inc}} \times 195.1/68 = \Delta f_{0,\text{Obs}} \times 195.1 / (-2.264 \times 10^{-6} \times 68 \times f_{0g}^2)$, where 195.1 in $\text{g}\cdot\text{mol}^{-1}$ is the molar weight of Pt, 68 in $\text{g}\cdot\text{mol}^{-1}$ is the net increased molar weight after displacing the Cu_{UPD} atoms with Pt atoms in the $2\text{Cu} + \text{PtCl}_6^{2-} = 2\text{Cu}^{2+} + 6\text{Cl}^- + \text{Pt}$ reaction ($68 = 195.1 - 2 \times 63.55$). Substituting $\Delta f_{0,\text{Obs}}$ (-36 Hz) into the above equation yields $\Delta m_{\text{Pt-Exptd}} = -36 \times 195.1 / (-2.264 \times 10^{-6} \times 68 \times 9000000^2) = 0.56 \mu\text{g}\cdot\text{cm}^{-2}$. The $\Delta m_{\text{Pt-Exptd}}$ here agrees well with relevant $\Delta m_{\text{Pt-exp}}$ obtained from separate “dry”-frequency QCM experiments ($0.54 \mu\text{g}\cdot\text{cm}^{-2}$), confirming the quantitative rationality of data given in Fig. S2.

(3) The replacement efficiency ($\eta_{\text{Pt-exp}}$) can be estimated according to the equation of $\eta_{\text{Pt-exp}} = n_{\text{Pt-exp}} / n_{\text{Cu-UPD}}$. From the above results of $\Delta m_{\text{Pt-exp}} = 0.54 \mu\text{g}\cdot\text{cm}^{-2}$ and $\Delta m_{\text{Cu-exp}} = 0.57 \mu\text{g}\cdot\text{cm}^{-2}$, we obtain $\eta_{\text{Pt-exp}} = (0.54/195.1)/(0.57/63.55) = 31\%$. From the above results of $\Delta m_{\text{Pt-Exptd}} = 0.56 \mu\text{g}\cdot\text{cm}^{-2}$ and $\Delta m_{\text{Cu-exp}} = 0.57 \mu\text{g}\cdot\text{cm}^{-2}$, we obtain $\eta_{\text{Pt-exp}} = (0.56/195.1)/(0.57/63.55) = 32\%$. Both $\eta_{\text{Pt-exp}}$ values as above are in good agreement with the $\eta_{\text{Pt-exp}}$ ($(30 \pm 3)\%$) for H_2PtCl_6 source in our work (Table 1), confirming again the quantitative rationality of data given in Fig. S2.

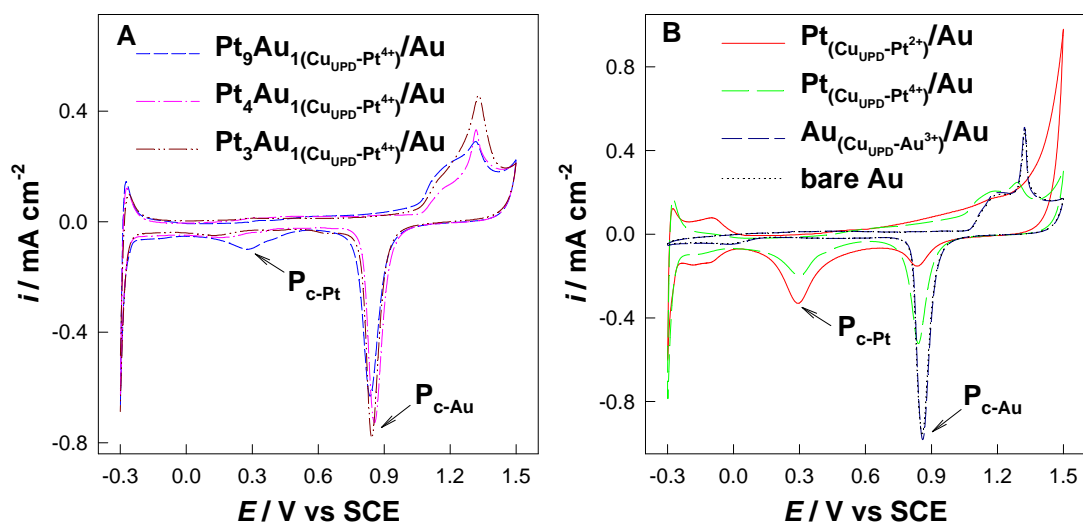


Fig. S3. Cyclic voltammograms of Pt₉Au₁(CuUPD-Pt⁴⁺)/Au, Pt₄Au₁(CuUPD-Pt⁴⁺)/Au, and Pt₃Au₁(CuUPD-Pt⁴⁺)/Au (A), as well as Pt_(CuUPD-Pt²⁺)/Au, Pt_(CuUPD-Pt⁴⁺)/Au, Au_(CuUPD-Au³⁺)/Au, and bare Au (B) in 0.1 M aqueous H₂SO₄. Scan rate: 50 $\text{mV} \cdot \text{s}^{-1}$.

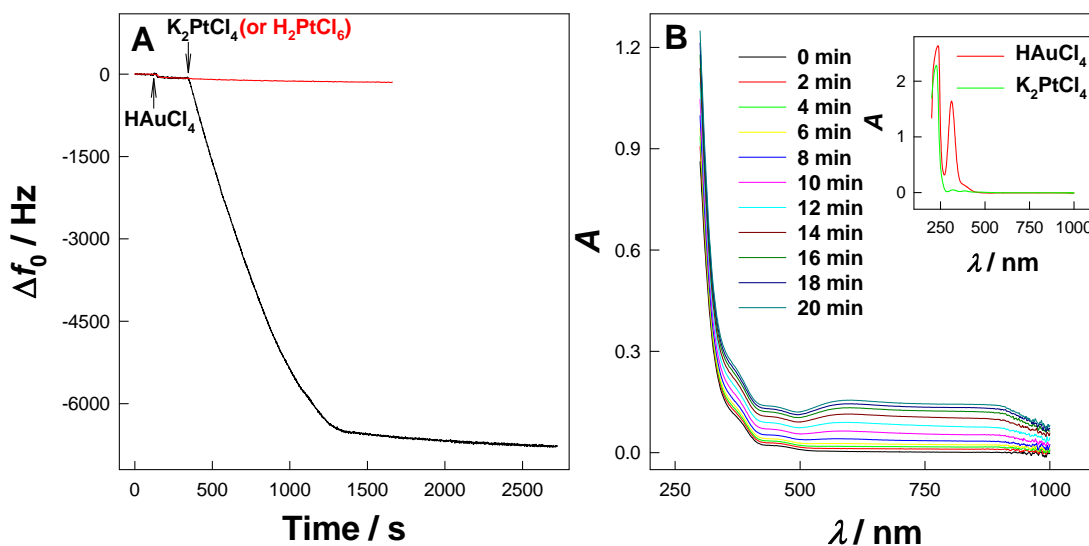


Fig. S4. (A) Time-dependent frequency responses on QCM Au electrode under open circuit potential to successive addition of 0.33 mM HAuCl_4 and then 0.67 mM K_2PtCl_4 (or 0.67 mM H_2PtCl_6 , red curve) into mildly stirred 0.1 M HClO_4 solution. All concentrations here are the final ones in the solution. (B) UV-vis absorption spectra of 0.33 mM HAuCl_4 + 0.67 mM K_2PtCl_4 solution after staying for different time lengths as labeled. Inset shows the UV-vis absorption spectra of 0.33 mM HAuCl_4 and 0.67 mM K_2PtCl_4 solution, respectively. Here, compared with the negligible decrease of f_0 after the addition of H_2PtCl_6 into HAuCl_4 solution, the much quicker decrease of f_0 after the addition of K_2PtCl_4 implies that the PtCl_4^{2-} can reduce AuCl_4^- to form Au nanoparticles, some of which can adhere to the Au electrode surface to decrease the frequency. In addition, the increase in the broad UV-vis absorption from 500 nm to 900 nm (light scattering by the generated Au nanoparticles) with the time increase also demonstrates the formation of Au nanoparticles with different size and morphology, which further proves that PtCl_4^{2-} can reduce AuCl_4^- .

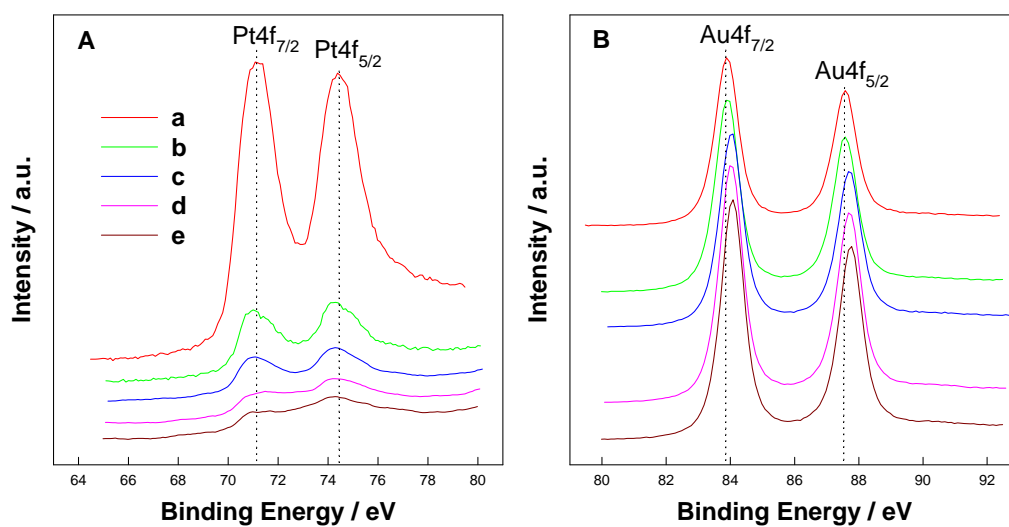


Fig. S5. XPS spectra of Pt4f (A) and Au4f (B) peaks for Pt_(CuUPD-Pt₂₊)/Au (a), Pt_(CuUPD-Pt₄₊)/Au (b), Pt₉Au_{1(CuUPD-Pt₄₊)}/Au (c), Pt₄Au_{1(CuUPD-Pt₄₊)}/Au (d), and Pt₃Au_{1(CuUPD-Pt₄₊)}/Au (e), respectively. Curve labels shown in Panel A are also for panel B. The dashed vertical lines are drawn to guide the eyes for more clearly discriminating the peak shift.

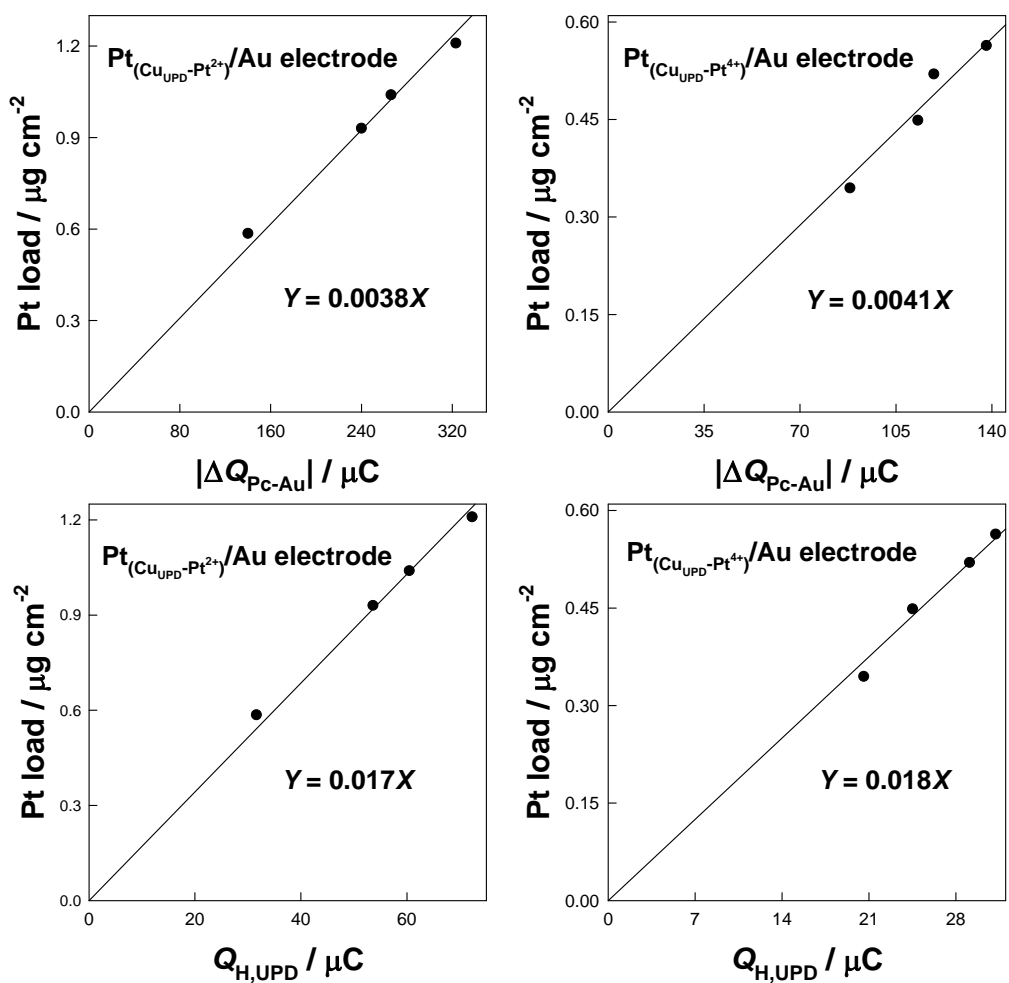


Fig. S6. The linear relationship between Pt load (calculated from QCM frequency responses) and $|\Delta Q_{\text{PC-Au}}|$ or $Q_{\text{H,UPD}}$ for $\text{Pt}_{(\text{CuUPD-Pt}^{2+})}/\text{Au}$ electrode or $\text{Pt}_{(\text{CuUPD-Pt}^{4+})}/\text{Au}$ electrode, respectively. The prepared electrodes were subjected to potential cycling ($50 \text{ mV}\cdot\text{s}^{-1}$, -0.3 – 1.5 V) in 0.1 M aqueous H_2SO_4 to obtain data of Pt-load-dependent $|\Delta Q_{\text{PC-Au}}|$ and H adsorption charge on Pt surface ($Q_{\text{H,UPD}}$), and $\Delta Q_{\text{PC-Au}}$ is the charge change under P_{C-Au} after Pt deposition on bare Au.

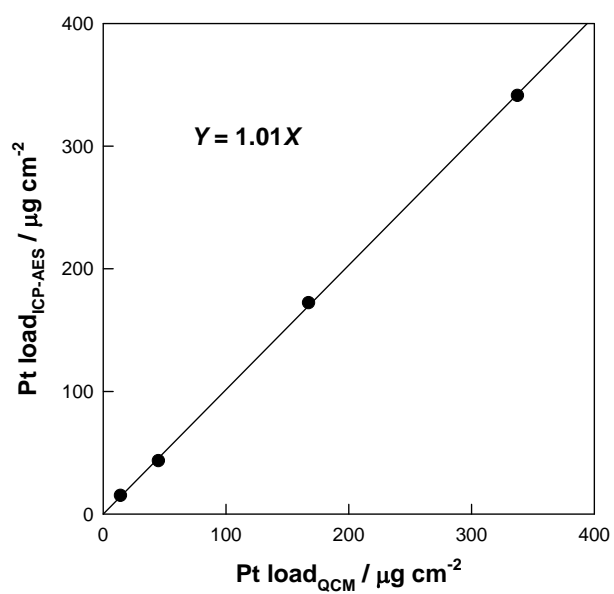


Fig. S7. The linear relationship between the Pt load_{ICP-AES} (from ICP-AES method) and the Pt load_{QCM} (from QCM method) of Pt_{pla}/Au electrodes.

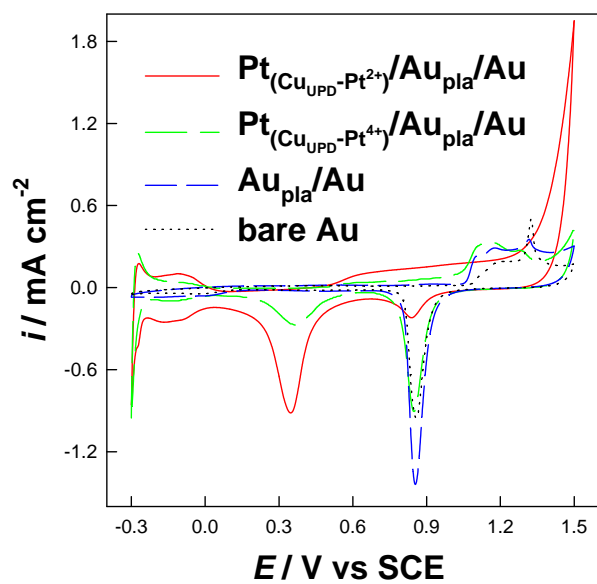


Fig. S8. Cyclic voltammograms of $\text{Pt}_{(\text{Cu}_{\text{UPD}}-\text{Pt}^{2+})}/\text{Au}_{\text{pla}}/\text{Au}$, $\text{Pt}_{(\text{Cu}_{\text{UPD}}-\text{Pt}^{4+})}/\text{Au}_{\text{pla}}/\text{Au}$, $\text{Au}_{\text{pla}}/\text{Au}$, and bare Au in 0.1 M aqueous H_2SO_4 . Scan rate: $50 \text{ mV} \cdot \text{s}^{-1}$.

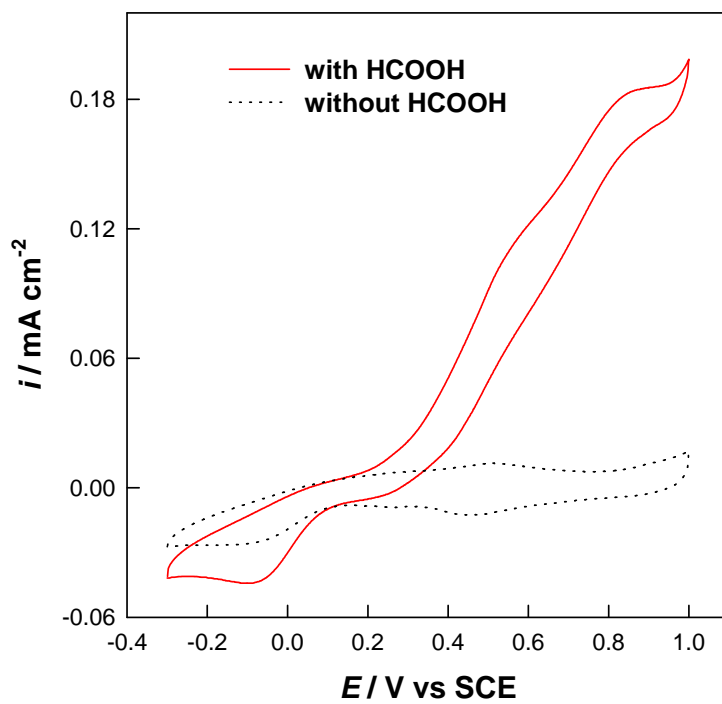


Fig. S9. Cyclic voltammograms of $\text{Au}_{(\text{CuUPD-Au}^{3+})}/\text{Au}$ in 0.1 M H_2SO_4 (dashed line) or 1 M $\text{HCOOH} + 0.1$ M H_2SO_4 (solid line) solution. Scan rate: $50 \text{ mV} \cdot \text{s}^{-1}$.

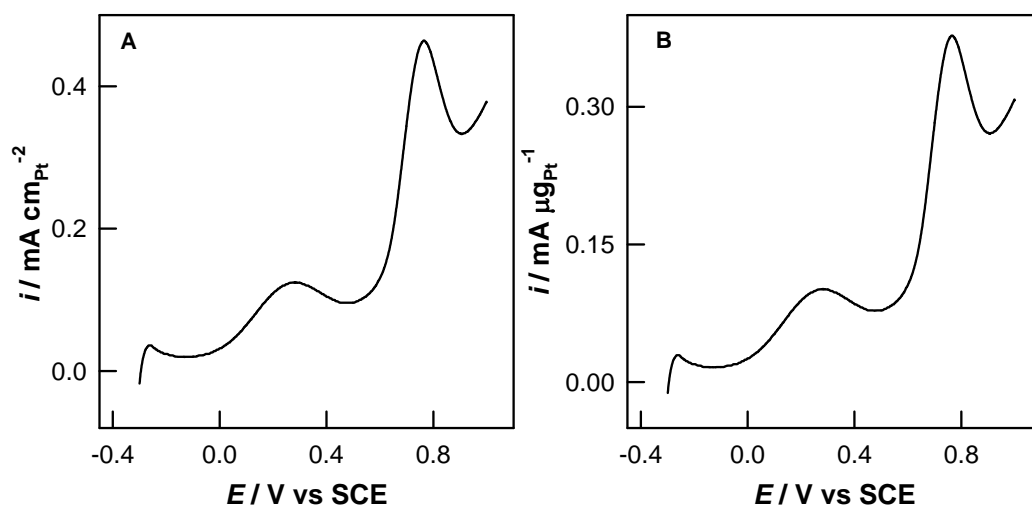


Fig. S10. Cyclic voltammograms of commercial E-TEK Pt/C (20%) in aqueous 1 M HCOOH + 0.1 M H₂SO₄. Currents in panels A and B are normalized to electroactive Pt surface area (from H UPD charge) and mass of Pt load, respectively. Scan rate: $50 \text{ mV} \cdot \text{s}^{-1}$.

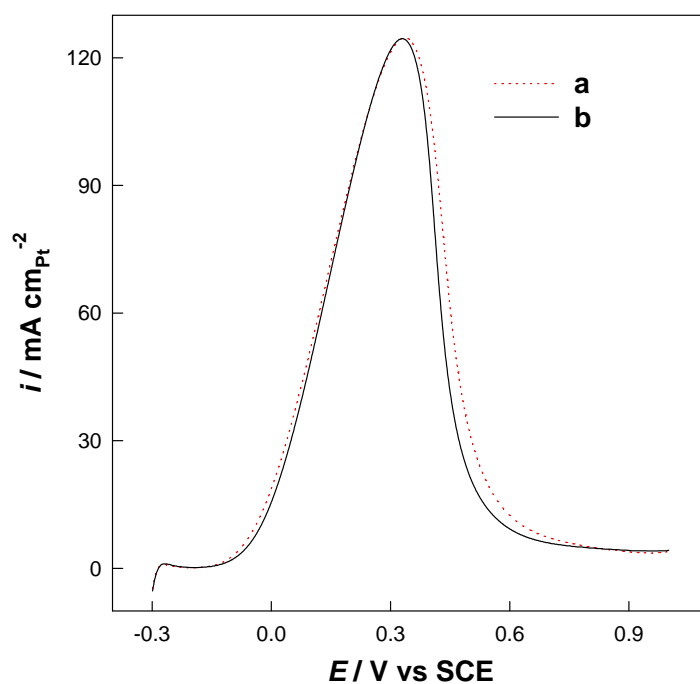


Fig. S11. Cyclic voltammograms of $\text{Pt}_4\text{Au}_1(\text{CuUPD-Pt}_4+)/\text{Au}(\text{CuUPD-Au}_3+)/\text{Au}$ (a, dashed line) and $\text{Pt}_4\text{Au}_1(\text{CuUPD-Pt}_4+)/\text{Au}$ (b, solid line) in 1 M HCOOH + 0.1 M H_2SO_4 solution. Scan rate: $50 \text{ mV} \cdot \text{s}^{-1}$. $\text{Pt}_4\text{Au}_1(\text{CuUPD-Pt}_4+)/\text{Au}(\text{CuUPD-Au}_3+)/\text{Au}$ was fabricated by modifying the $\text{Au}(\text{CuUPD-Au}_3+)/\text{Au}$ electrode with a full monolayer of Cu_{UPD} followed by its redox replacement with noble metal atoms in 0.8 mM H_2PtCl_6 + 0.2 mM HAuCl_4 + 0.1 M HClO_4 solution.

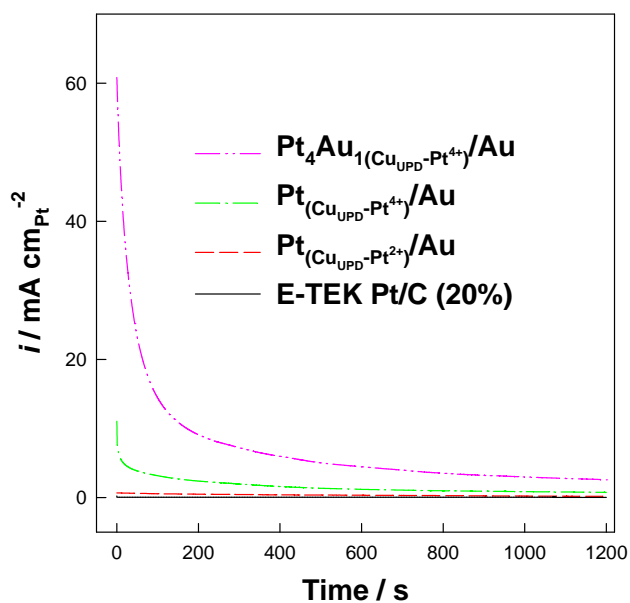


Fig. S12. The i - t curves at 0.1 V of $\text{Pt}_4\text{Au}_1(\text{Cu}_{\text{UPD}}\text{-Pt}^{4+})/\text{Au}$, $\text{Pt}_{(\text{Cu}_{\text{UPD}}\text{-Pt}^{4+})}/\text{Au}$, $\text{Pt}_{(\text{Cu}_{\text{UPD}}\text{-Pt}^{2+})}/\text{Au}$ and commercial E-TEK Pt/C (20%) in 1 M HCOOH + 0.1 M H_2SO_4 solution.

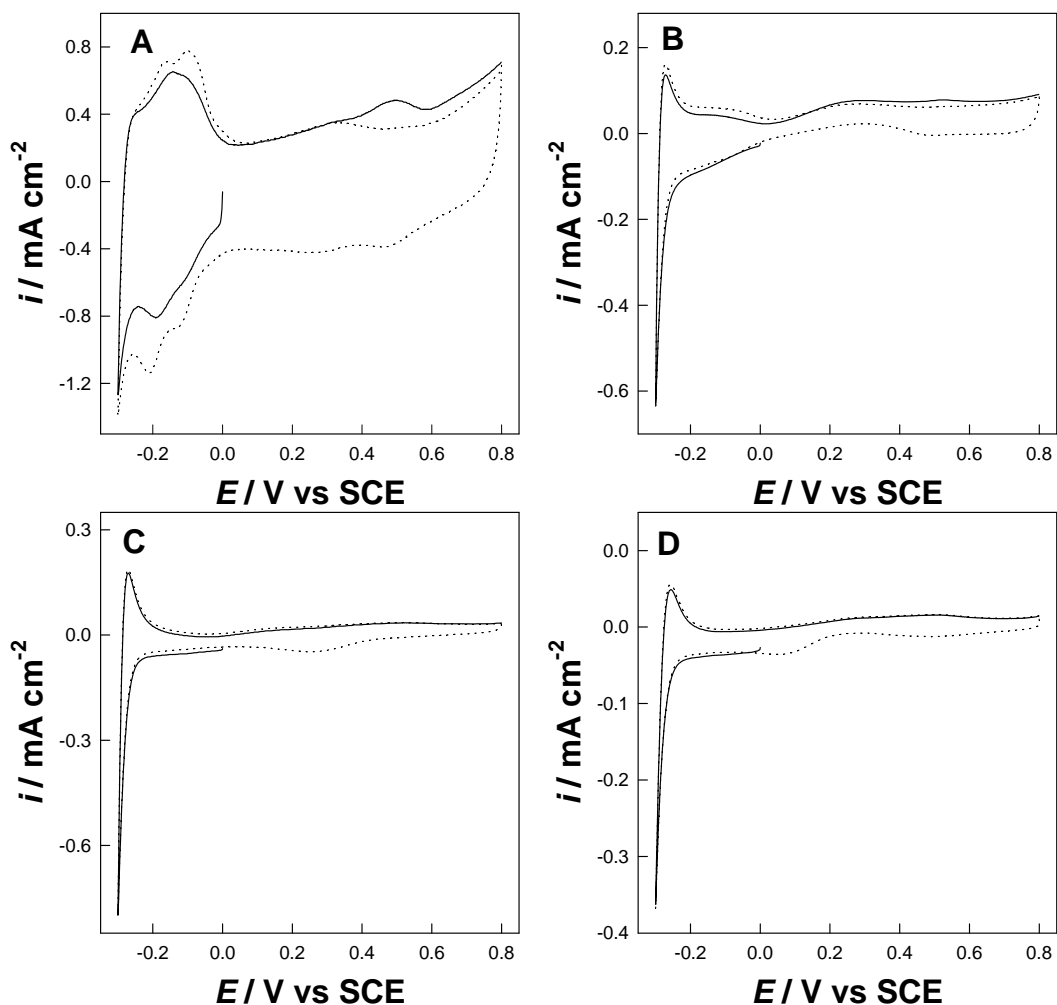


Fig. S13. Cyclic voltammograms in 0.1 M H₂SO₄ for stripping of the CO_{ads} poison which was formed on (A) commercial E-TEK Pt/C (20%), (B) Pt_(CuUPD-Pt2+)/Au, (C) Pt_(CuUPD-Pt4+)/Au, or (D) Pt₄Au_{1(CuUPD-Pt4+)}/Au under open circuit potential in 1 M HCOOH. The solid lines show the first positive sweeps while the dashed lines show the subsequent sweeps upon removal of the poisonous species. Scan rate: 50 mV·s⁻¹. Here, the big oxidation peak on the commercial E-TEK Pt/C (20%) at 0.5 V in the first positive potential sweep is ascribed to the oxidation of CO_{ads}.^{S3} Only a weak oxidation peak of CO_{ads} at 0.52 V occurs on Pt_(CuUPD-Pt2+)/Au, whereas the peak vanishes on Pt_(CuUPD-Pt4+)/Au and Pt₄Au_{1(CuUPD-Pt4+)}/Au, proving the direct oxidation of FA on noncontinuous/isolated Pt overlayer without generating CO_{ads}.

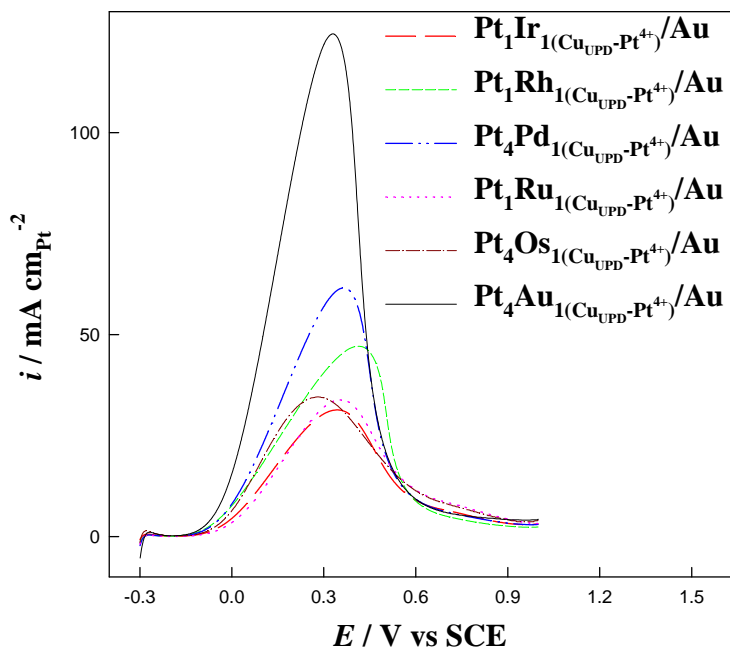


Fig. S14. Cyclic voltammograms of $\text{Pt-M}_{(\text{Cu}_{\text{UPD}}\text{-Pt}^{4+})}/\text{Au}$ and $\text{Pt}_4\text{Au}_1(\text{Cu}_{\text{UPD}}\text{-Pt}^{4+})/\text{Au}$ in 1 M HCOOH + 0.1 M H_2SO_4 solution. Scan rate: $50 \text{ mV} \cdot \text{s}^{-1}$. $\text{M}=\text{Ir, Rh, Pd, Ru, and Os}$. The optimal molar concentration ratio of the Pt salt (H_2PtCl_6) to another noble metal (M) salt in each of the mixed solutions for preparation of Pt-M MAMEC is marked here by the numerical subscripts.

References

- S1. X. M. Tu, Q. J. Xie, C. H. Xiang, Y. Y. Zhang and S. Z. Yao, *J. Phys. Chem. B*, 2005, **109**, 4053.
- S2. N. Tian, Z. Y. Zhou, S. G. Sun, Y. Ding and Z. L. Wang, *Science*, 2007, **316**, 732.
- S3. M. J. Llorca, J. M. Feliu, A. Aldaz and J. Clavilier, *J. Electroanal. Chem.*, 1994, **376**, 151.
- S4. C. H. Wang, C. Yang, Y. Y. Song, W. Gao, and X. H. Xia, *Adv. Funct. Mater.*, 2005, **15**, 1267.
- S5. Handbook of X-ray Photoelectron Spectroscopy, J. F. Moulder, W. F. Tickle, P. E. Sobol, K. D. Bomben, Eds., Physical Electronics, Inc.: Eden Prairie, 1995.
- S6. G. R. Zhang, D. Zhao, Y. Y. Feng, B. S. Zhang, D. S. Su, G. Liu and B. Q. Xu, *ACS Nano*, 2012, **6**, 2226.
- S7. Z. H. Zhang, Y. Wang and X. G. Wang, *Nanoscale*, 2011, **3**, 1663.
- S8. D. Zhao, Y. H. Wang and B. Q. Xu, *J. Phys. Chem. C*, 2009, **113**, 20903.
- S9. S. Zhang, Y. Y. Shao, G. P. Yin and Y. H. Lin, *Angew. Chem. Int. Ed.*, 2010, **49**, 1.
- S10. S. Zhang, Y. Y. Shao, G. P. Yin and Y. H. Lin, *J. Power Sources*, 2010, **195**, 1103.
- S11. S. Zhang, S. J. Guo, H. Y. Zhu, D. Su and S. H. Sun, *J. Am. Chem. Soc.*, 2012, **134**, 5060.
- S12. Kim, C. Jung, J. Kim, C. K. Rhee, S. Choi and T. Lim, *Langmuir*, 2010, **26**, 4497.
- S13. J. Kim, C. Jung, C. K. Rhee, and T. Lim, *Langmuir*, 2007, **23**, 10831.